RESEARCH ARTICLE

Research on Tractor Active Seat Suspension Based on Model Predictive Control

**SIXIA ZHAO, (Member, IEEE), GUANGCHAO QU, (Member, IEEE),
MENGNAN LIU, (Member, IEEE), XIAOLIANG CHEN, (Member, IEEE),
ZHI GAO, (Member, IEEE), AND LIYOU XU, (Member, IEEE)**

Vehicle & Transportation Engineering Institute, Henan University of Science and Technology, Luoyang 471003, China
State Key Laboratory of Intelligent Agricultural Power Equipment, Luoyang 471003, China
School of Vehicle and Traffic Engineering, Henan Institute of Technology, Xinxiang 453000, China

Corresponding author: Liyou Xu (xlyou@haust.edu.cn)

ABSTRACT In order to reduce the influence of ground vibration generated by tractors during driving and operation on driving stability and driver 's ride comfort, this paper proposes a tractor active seat suspension control method based on model predictive control (MPC). Through the establishment of three degrees of freedom tractor active seat suspension model, electromagnetic actuator (linear motor) model and ground excitation input model, the inner and outer loop control strategy of linear motor active seat suspension based on outer loop MPC control and inner loop current hysteresis comparison control is proposed. The influence of MPC parameters on the vibration performance and control cost of seat suspension is compared and analyzed through experiments. The appropriate system parameters are selected through optimization analysis. The simulation and experimental results show that compared with the passive seat suspension and PID seat suspension, the tractor active seat suspension based on model predictive control improves the ride comfort and vibration reduction characteristics of the tractor, and on this basis, it reduces the energy consumption required for the seat suspension system to achieve active control, while ensuring the timeliness of MPC control.

INDEX TERMS Tractor, active seat suspension, MPC, vibration damping, ride comfort.

I. INTRODUCTION

Usually, vibration will bring serious health problems to human beings. Drivers of heavy vehicles, such as tractors, bulldozers, loaders, etc., will face more risks. By studying the seat suspension with good vibration reduction performance and scientific and effective control algorithms, the vibration transmitted from the road surface to the human body can be effectively reduced, thereby reducing the impact of vibration on human health. Tractors usually operate in fields with high road excitation, which exposes the tractor driver to various vibration levels. Long-term vibration can cause

The associate editor coordinating the review of this manuscript and approving it for publication was Nasim Ullah.

serious damage to the driver 's body [1], [2]. Factors such as road roughness, tires, seat suspension systems, and full-body vibration affect the driver 's ride comfort [3]. How to effectively improve the ride comfort of tractors without increasing input costs is one of the key issues currently faced by various agricultural machinery enterprise. The vibration generated by the tractor during driving and operation is finally transmitted to the human body through the seat suspension, which can minimize the vibration impact transmitted to the human body [4]. It is easy to adjust the seat structure and parameters. It has the advantages of short manufacturing cycle, quick effect, practical economy, convenience and feasibility, and does not affect the other performance of the vehicle while changing the dynamic characteristics of the seat suspension

system. In short, it is more practical and economical to study the tractor seat suspension system and improve its vibration isolation performance [5].

Compared with the passive seat suspension system, the structure and control of the active seat suspension system are more complex, and the actuator outputs the active force completely according to the requirements of the control strategy. Therefore, it is the key to choose a scientific and effective control strategy to improve the performance of the tractor seat suspension. At present, the control strategies for active seat suspension include traditional PID control, linear quadratic regulator (LGR), fuzzy logic controller (FLC), artificial neural network (ANN), H_∞ and sliding mode controller (SMC) [6]. In addition, many researchers have also designed hybrid controllers such as PID-FLC and SMC-PI. The H_∞ optimal controller based on sliding mode observer designed by Wang et al. [7] can accurately estimate the unknown disturbance of the seat suspension system, and improve the performance index of the seat suspension and the driver's ride comfort. Sha et al. [8] used the adaptive learning function of BP neural network to integrate the control parameters of the traditional PID seat suspension in real time by collecting the deviation signal, so that the seat suspension has better adaptability and damping effect. Shu Ma et al. [9] studied a PID control method of active seat suspension system based on low-pass filtering, which effectively improved the performance index of active seat suspension system. Luan et al. [10] proposed a VEI-VD device and a semi-active control strategy. In the random excitation test, the root mean square value of the seat acceleration is effectively reduced and the ride comfort is improved. Olivier and Woo [11] used the Skyhook controller to control the current supply of the hybrid magnetorheological damper and enhance the damping force under low current power supply. The skyhook controller improves seat comfort compared to uncontrolled conditions. Xuan et al. [12] proposed a new switch adaptive fuzzy controller, and used a car seat suspension with a controllable magnetorheological damper to verify the robustness and effectiveness of the proposed controller in the corresponding road excitation and external disturbance. The results show that the controller has better vibration control performance than the existing robust controller, and the displacement and speed at the seat position are well reduced.

MPC is a very successful and mature control scheme in recent decades, and has been widely used in various fields [13]. Narayan et al. [14] studied LQR and MPC control strategies, and the quadratic cost function of the two control schemes optimized the state variables and input variables, and used MATLAB-SIMULINK to simulate and compare the ride comfort index and actuator power. The results show that the suspension performance and power requirements of MPC are significantly improved compared with LQR on both road grades. MPC reduces the actuator power consumption requirements, actuator size and weight. Maciejewski et al. [15] designed a controller with adaptive mass identification

function. The adaptive mechanism identifies the actual load mass to improve the vibration isolation effect and enhance the robustness of the system when the mass load response changes. Myron et al. [16] proposed a road preview model predictive controller combined with radial basis function model as the control scheme of the whole vehicle active suspension system. The RBF model adopted can effectively approximate the nonlinear behavior of the suspension system, thus improving the performance of the linear MPC method. Kun et al. [17] considered the physical constraints of the electromagnetic actuator and the dynamic deflection stroke of the suspension. Based on the model predictive control method, a 1/4 vehicle electromagnetic active suspension controller was designed, and the instantaneous vertical impact and random uneven road conditions were simulated and analyzed. The results show that compared with the LQR active suspension, the model predictive control can improve the ride comfort performance of the vehicle. Zhao and Yin [18] designed a model predictive controller for the active suspension driven by electro-hydraulic servo. The simulation results show that the vertical acceleration of the body, the dynamic deflection of the suspension and the dynamic load of the tire are greatly reduced, and the damping effect is obvious. The model predictive controller has strong robustness under parameter changes and road disturbances. MPC is a control scheme that can adapt to the nonlinearity of the object. It has excellent dynamic response ability and small energy consumption, and is suitable for active seat suspension.

Traditional control algorithms such as PID can only consider various constraints of system input and output variables, while MPC control can consider various constraints of spatial state variables, such as displacement of seat suspension system, vertical vibration velocity of human body, vertical vibration velocity of vehicle body, displacement of unsprung mass, vertical vibration velocity of unsprung mass, etc. The traditional control algorithm adopts an invariant global optimization goal. The optimization process is carried out offline, and it cannot effectively deal with external disturbances in the control process. However, there are some uncertainties and external disturbances in the process of driving and working of tractors, including the change of working state and the change of driving road environment and seat load quality. MPC control algorithm adopts the finite time domain optimization strategy of time forward rolling, which can be carried out repeatedly online, and has strong adaptability to this uncertainty and external interference. The state information and constraints of each control cycle of the seat suspension system can be optimized online in the finite prediction domain, so that the controller can maintain the optimal control at each moment, which can provide better control effect for the tractor active seat suspension system. But at the same time, control time and energy consumption will also increase. Therefore, it is urgent to study a new and effective control algorithm to solve the above problems, so as to realize the optimal control of the damping effect of the seat suspension
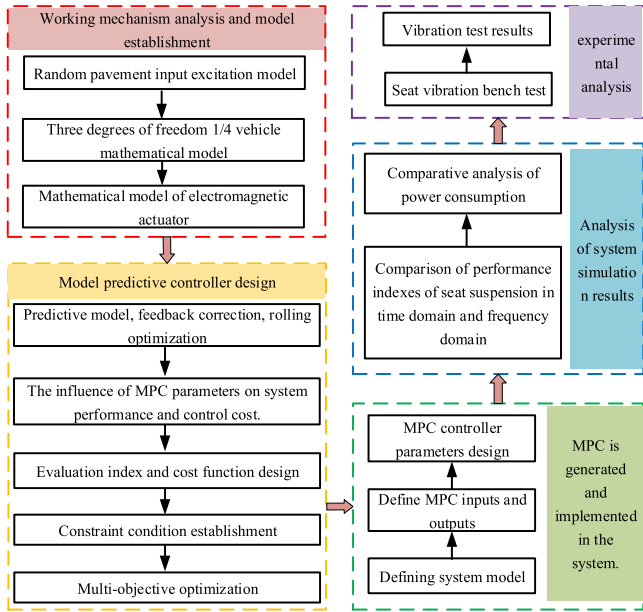
FIGURE 1. MPC active seat suspension research technology roadmap.

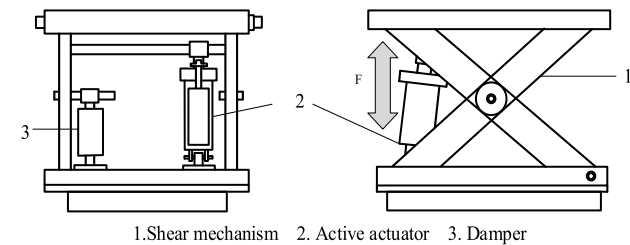1.Shear mechanism   2. Active actuator   3. Damper

FIGURE 2. Structure diagram of active seat suspension.

system. At the same time, the study of the energy consumption and control timeliness of the control system is crucial for the future popularization of active seat suspension systems in agricultural machinery such as tractors, because it is related to the cost issue.

The realization of active control of MPC seat suspension system is more complicated. This paper first realizes the main goal of optimal control of vibration reduction effect of the system. On this basis, the energy consumption and control timeliness of the system are studied. In this paper, based on the 1/4 vehicle model, a new element-electromagnetic actuator is added to the mechanical basis of the passive seat suspension, and the inner and outer loop closed control system is designed. MPC active power control scheme and electromagnetic actuator have not been applied in agricultural tractor seat suspension. Aiming at the problem of long control time caused by MPC online repeated optimization, the influence of MPC parameters on seat suspension vibration performance and control cost is analyzed through experiments. Based on the sampling time, prediction time domain and control time domain determined by the experiment, the weight matrix of MPC controller is optimized to realize the optimal control effect, energy consumption and timeliness of MPC active seat suspension system.
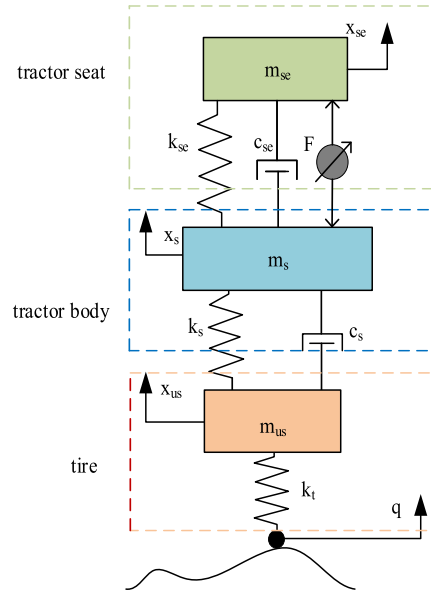

FIGURE 3. Three degrees of freedom 1 / 4 vehicle model.

The rest of this article is organized as follows: Section II establishes a system model and analyzes the working mechanism of the system. Section III includes the design and optimization analysis of the model predictive controller. Section IV includes the analysis of simulation and experimental results. Finally, the conclusion is drawn in Section V. Figure 1 shows the detailed work of this paper.

II. ESTABLISHMENT OF TRACTOR ACTIVE SEAT SUSPENSION SYSTEM MODEL

A. MATHEMATICAL MODEL OF ACTIVE SEAT SUSPENSION SYSTEM

In this paper, the widely used scissor seat structure is taken as an example for dynamic analysis, and its structure is X-shaped. Actuators can be divided into three categories: hydraulic, pneumatic and servo actuators [19]. As shown in Figure 2, the seat base is fixed on the vehicle cockpit floor, and the roof is connected to the seat chassis. The active actuator is placed in the inner shear structure, and the upper and lower ends of the active actuator are connected to the upper and lower plates of the seat base. The active seat suspension system with scissor mechanism is driven by an active actuator in the vertical direction, and the active actuator is used in parallel with the damper to absorb and reduce the vibration impact in the vertical direction [20].

The seat suspension model is the basis for the design of the active seat suspension controller. In engineering applications, a simplified system model is usually used to describe the controlled object [21].

In engineering applications, a simplified system model is usually used to describe the controlled object. In this paper, the vertical vibration of tractor seat suspension is studied. The tractor is simplified as a 1/4 vehicle model with three degrees of freedom [22], [23]. The tractor seat and the human body are assumed to be a single-degree-of-freedom system as a whole.

Figure 3 shows the active seat suspension that integrates a 1/4 vehicle model and an active actuator fixed in parallel with the suspension.

The tire damping can be ignored and simplified as a constant coefficient stiffness spring k_t. Assuming that both the seat suspension and the vehicle suspension have linear characteristics, the dynamic equation is [24]:

$$m_{se}\ddot{x}_{se} = -k_{se}(x_{se} - x_s) - c_{se}(\dot{x}_{se} - \dot{x}_s) + F$$
$$m_s\ddot{x}_s = k_{se}(x_{se} - x_s) - c_s(\dot{x}_s - \dot{x}_{us}) - k_s(x_s - x_{us}) - F$$
$$m_{us}\ddot{x}_{us} = c_s(\dot{x}_s - \dot{x}_{us}) + k_s(x_s - x_{us}) - k_t(x_{us} - q) \quad (1)$$

where m_{se} is the combined mass of human and seat; m_s is the body mass; m_{us} is the unsprung mass. Their displacements in the vertical direction are x_{se}, x_s and x_{us}, respectively. q is random road excitation displacement; k_{se}, c_{se} is the stiffness coefficient and damping coefficient of seat suspension spring; k_s, c_s is the stiffness coefficient and damping coefficient of the tractor body; F is active control force.

F and q are used as control vectors. Taking $x_{se}, \dot{x}_{se}, x_s, \dot{x}_s,$ $x_{us}, \dot{x}_{us}$ as the state variables of the system. $x_{se}, \dot{x}_{se}, x_s, \dot{x}_s, \ddot{x}_{se},$ $x_{se} - x_s$ as the output variables.

$$x = \begin{bmatrix} x_{se} & \dot{x}_{se} & x_s & \dot{x}_s & x_{us} & \dot{x}_{us} \end{bmatrix}^T$$
$$y = \begin{bmatrix} x_{se} & \dot{x}_{se} & x_s & \dot{x}_s & \ddot{x}_{se} & x_{se} - x_s \end{bmatrix}^T$$

Then the state space equation of the system model corresponding to Equation 1 can be expressed as:

$$\begin{cases} \dot{x} = Ax + Bu \\ y = Cx + Du \end{cases} \quad (2)$$

where A is the coefficient matrix of the state vector; B is the input coefficient matrix; C is the output coefficient matrix of the state vector; D is the output coefficient matrix; u is the input vector;

$$A = \begin{bmatrix} 0 & 1 & 0 & 0 & 0 & 0 \\ \frac{-k_{se}}{m_{se}} & \frac{-c_{se}}{m_{se}} & \frac{k_{se}}{m_{se}} & \frac{c_{se}}{m_{se}} & 0 & 0 \\ 0 & 0 & 0 & 1 & 0 & 0 \\ \frac{k_{se}}{m_s} & \frac{c_{se}}{m_s} & \frac{-(k_{se}+k_s)}{m_s} & \frac{-(c_{se}+c_s)}{m_s} & \frac{k_s}{m_s} & \frac{c_s}{m_s} \\ 0 & 0 & 0 & 0 & 0 & 1 \\ 0 & 0 & \frac{k_s}{m_{us}} & \frac{c_s}{m_{us}} & \frac{-(k_t+k_s)}{m_{us}} & \frac{-c_s}{m_{us}} \end{bmatrix}$$

$$C = \begin{bmatrix} 1 & 0 & 0 & 0 & 0 & 0 \\ 0 & 1 & 0 & 0 & 0 & 0 \\ 0 & 0 & 1 & 0 & 0 & 0 \\ 0 & 0 & 0 & 1 & 0 & 0 \\ \frac{-k_{se}}{m_{se}} & \frac{-c_{se}}{m_{se}} & \frac{k_{se}}{m_{se}} & \frac{c_{se}}{m_{se}} & 0 & 0 \\ \frac{k_{se}}{m_s} & \frac{c_{se}}{m_s} & \frac{-(k_{se}+k_s)}{m_s} & \frac{-(c_{se}+c_s)}{m_s} & \frac{k_s}{m_s} & \frac{c_s}{m_s} \end{bmatrix}$$

$$B = \begin{bmatrix} 0 & 0 \\ \frac{-1}{m_{se}} & 0 \\ 0 & 0 \\ \frac{1}{m_s} & 0 \\ 0 & 0 \\ 0 & \frac{k_t}{m_{us}} \end{bmatrix} \quad D = \begin{bmatrix} 0 & 0 \\ 0 & 0 \\ 0 & 0 \\ 0 & 0 \\ \frac{-1}{m_{se}} & 0 \\ \frac{-1}{m_s} & 0 \end{bmatrix} \quad u = \begin{bmatrix} F \\ q \end{bmatrix}$$

B. MATHEMATICAL MODEL AND CONTROL OF ELECTROMAGNETIC ACTUATOR FOR ACTIVE SEAT SUSPENSION

1) MATHEMATICAL MODEL OF ELECTROMAGNETIC ACTUATOR

The distribution of magnetomotive force and magnetic field of linear motor is similar to that of rotating motor. It can be studied by referring to permanent magnet synchronous rotating motor. It is assumed that the winding is ideally distributed, the magnetic field of permanent magnet is stable, and the harmonic and magnetic saturation effects are not considered [25]. The motor model of linear motor in a, b, c coordinate is:

$$\begin{bmatrix} \psi_a \\ \psi_b \\ \psi_c \end{bmatrix} = \begin{bmatrix} L_{aa} & M_{ab} & M_{ac} \\ M_{ba} & L_{bb} & M_{bc} \\ M_{ca} & M_{cb} & L_{cc} \end{bmatrix} \begin{bmatrix} i_a \\ i_b \\ i_c \end{bmatrix}$$
$$+ \psi_{PM} \begin{bmatrix} \cos\theta \\ \cos(\theta - \frac{2\pi}{3}) \\ \cos(\theta + \frac{2\pi}{3}) \end{bmatrix} \quad (3)$$

$$\begin{cases} u_a = R_s i_a + \dfrac{d\psi_a}{dt} \\ u_b = R_s i_b + \dfrac{d\psi_b}{dt} \\ u_c = R_s i_c + \dfrac{d\psi_c}{dt} \end{cases} \quad (4)$$

where ψ_a, ψ_b, ψ_c is three-phase flux; L_{aa}, L_{bb}, L_{cc} is the self-inductance coefficient of the motor stator winding; i_a, i_b, i_c is three-phase current; ψ_{PM} is flux linkage; $M_{ab}, M_{ac}, M_{ba}, M_{bc}, M_{ca}, M_{cb}$ is the mutual inductance coefficient of stator winding; τ is polar distance; u_a, u_b, u_c is three-phase voltage; R_s is stator resistance.

It is difficult to analyze and control the permanent magnet synchronous linear motor in a, b, c coordinate system, because the flux linkage changes with the relative position between the stator and the mover of the motor, and the torque equation involves the current vector and flux linkage equation of the linear motor, which is more complicated. The above equations of voltage, current and flux linkage are transformed into $d - q$ coordinate system, so that the d-axis and q-axis are decoupled to realize vector control, and the mathematical model of linear motor in $d - q$ coordinate system is established:

Stator voltage equation:

$$\begin{bmatrix} u_d \\ u_q \end{bmatrix} = \begin{bmatrix} R_s & 0 \\ 0 & R_s \end{bmatrix} \begin{bmatrix} i_d \\ i_q \end{bmatrix} + \begin{bmatrix} \dot{\psi}_d - \omega_r \psi_q \\ \dot{\psi}_d + \omega_r \psi_d \end{bmatrix}$$
$$\begin{cases} u_d = R_s i_d + \dfrac{d\psi_d}{dt} - \omega_r \psi_q \\ u_q = R_s i_q + \dfrac{d\psi_q}{dt} + \omega_r \psi_d \end{cases} \quad (5)$$

The stator flux equation:

$$\psi_d = L_d i_d + \psi_{PM}$$
$$\psi_q = L_q i_q \quad (6)$$

where u_d, u_q is the stator voltage of $d - q$ axis; ψ_d, ψ_q is the flux linkage vector of $d - q$ axis. ω_r is the equivalent angular velocity of permanent magnet synchronous linear motor.

The electromagnetic thrust expression of permanent magnet synchronous linear motor is:

$$F_e = \frac{P_e}{v_m} = \frac{3}{2} n_p \frac{\pi}{\tau} \left[\psi_{PM} i_q + (L_d - L_q) i_d i_q \right] \qquad (7)$$

where F_e is the electromagnetic thrust; ψ_{PM} is the permanent magnet flux linkage.

The mechanical motion equation of linear motor is:

$$m \frac{dv}{dt} = F_e - B v_m - F_f - F_z - F_d \qquad (8)$$

where F_z is load resistance; F_d is external disturbance; F_f is friction; B is the friction coefficient.

In order to simplify the complexity of linear motor control, this paper adopts the current hysteresis comparison control method, and sets the $d-$ axis excitation current $i_d = 0$ thus simplifying the above equation to obtain the linear function relationship between the permanent magnet synchronous linear motor and the quadrature-axis stator current [26]:

$$F_e = \frac{3\pi}{2\tau} n_p \psi_{PM} i_q = k_i i_q \qquad (9)$$

where F_e is the electromagnetic thrust; k_i is the electromagnetic thrust coefficient, which is a constant related to the parameters of the linear motor itself.

It can be seen that the electromagnetic thrust of the permanent magnet synchronous linear motor is proportional to the current i_q. By controlling the size of the $q-$ axis current i_q, the size of the electromagnetic thrust F_e of the permanent magnet synchronous linear motor can be controlled.

2) CURRENT HYSTERESIS COMPARISON CONTROL OF ELECTROMAGNETIC ACTUATOR

The principle of the current hysteresis comparison controller is to make the actual current of the three-phase winding track the target current required by the motor, and make the error between the two within a certain range. The current hysteresis comparison control principle is shown in Figure 4. By comparing the target current with the actual current, the PWM signal generated by the controller realizes the on-off control of the components to realize the control of the three-phase winding current of the linear motor. It can be seen from Equation (9) that the thrust of the permanent magnet synchronous linear motor is linearly proportional to the stator current i_q, so the control of the electromagnetic thrust is realized by controlling the current i_q.

The current hysteresis comparison control current comparison results are shown in Figure 5. In the range of $i + \Delta i$ and $i - \Delta i$, the actual current i effectively tracks the target current i^*.

The linear motor model is established by the above formulas. The input of the motor model is three-phase current. After Clark transformation and Park transformation, the current of the under the $d - q$ axis two-phase rotating shaft system is
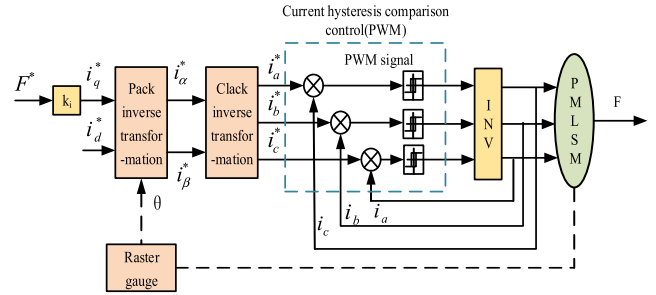

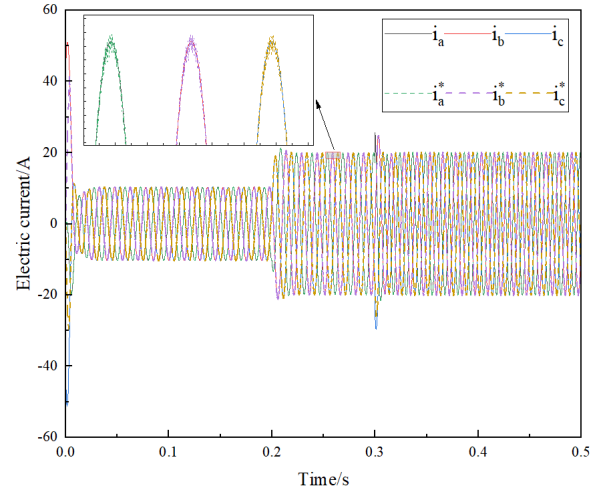**FIGURE 4.** Current hysteresis comparison control schematic diagram.

FIGURE 5. Current hysteresis comparison control current comparison results.

obtained. According to formula (7) $\sim$ (9), the active power F required by the seat suspension system is obtained, which acts on the seat suspension system.

III. DESIGN OF ACTIVE SEAT SUSPENSION CONTROLLER
A. PID CONTROLLER DESIGN

Due to the simple and reliable characteristics of PID controller, it is widely used in seat suspension control. The PID controller is composed of proportional, integral and derivative controllers. The control principle is shown in Figure 6, where e is the difference between the ideal value and the actual value of the controlled object. The outer ring control of the seat suspension adopts the conventional PID controller, and the PID parameters are set to realize the control of the vertical acceleration of the driver's seat. In this study, the controller parameters were set by trial and error method. With reference to the adjustment characteristics of the PID controller, the parameters are determined by observing the control effect after changing the PID parameters. When adjusting, the value of the proportional parameter is gradually increased, the change of the control curve is observed, and the optimal value is selected. The adjustment of the integral coefficient is the same as that of the proportional coefficient. With the change of control effect, it is also adjusted from small to large. If the control effect is not ideal, the influence of the derivative coefficient in the control strategy should be considered. The adjustment method of derivative parameters is the same as
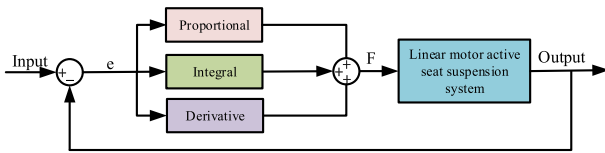
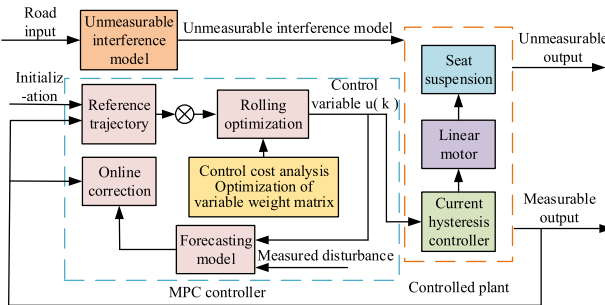**FIGURE 6.** PID control principle diagram.

FIGURE 7. Active seat suspension model predictive control system structure diagram.

that of proportional and integral parameters. From small to large, the proportional parameters and integral parameters are fine-tuned at the same time, and the values of the three parameters are adjusted repeatedly to obtain the ideal control effect. Finally, the PID parameters $K_p = 100, K_i = 250, K_d = 0.1$ are selected.

The transfer function of PID controller is [27]:

$$G_c(s) = K_p + \frac{K_i}{s} + K_d s \tag{10}$$

where K_p is the proportional parameter, $K_p = 100$; K_i is the derivative parameter, $K_i = 250$; K_d is the integral parameter, $K_d = 0.1$;

B. MPC CONTROLLER DESIGN
1) MPC ACTIVE SEAT SUSPENSION CONTROL PRINCIPLE
The basic idea of model predictive control is to predict the future output of the system by using the existing model, the current state of the system and the future control area. The MPC active seat suspension system predicts the future output (human-seat vibration acceleration and dynamic deflection) of the seat suspension system based on the current state variables (human-seat displacement, vibra-

tion velocity and body displacement, vibration velocity) and future input (actuator active force and road excitation). The control objective is achieved by rollingly solving constrained optimization problems. Solving the optimization problem in the moving time range and having a long predictive ability are the most important characteristics of MPC that distinguish it from other control methods [28], [29]. Figure7 shows the structure of the tractor active seat predictive control system.

2) FORECASTING MODEL
Model predictive control solves the optimal problem in the discrete time domain by aiming at the state and constraint conditions of each control period, so that the controller remains optimal at each moment. Therefore, it is necessary to discretize the existing continuous-time state equation (2).

$$\frac{x(k+1) - x(k)}{T_s} = Ax(k) + Bu(k)$$
$$y(k) = Cx(k) + Du(k) \tag{11}$$

The discretized state equation can be expressed as:

$$\begin{cases} x(k+1) = A_c x(k) + B_c x(k) \\ y(k) = C_c x(k) + D_c u(k) \end{cases} \tag{12}$$

where T_s is the sampling time; is the coefficient matrix of discrete system A_c, B_c, C_c, D_c under sampling period; k is the discrete time of the system.

The tractor seat suspension simulation parameters in table 4 are brought into the expression (2), and the coefficient matrix A of the state vector, the input coefficient matrix B, the output coefficient matrix C of the state vector, and the specific value of the output coefficient matrix D are obtained. Using the c2d function in MATLAB, the coefficient matrix can be discretized by setting the sampling time, where the discrete time $T_s = 0.01$. Then the discrete model matrix A_c, B_c, C_c, D_c can be obtained as shown at the bottom of the page.

3) ROLLING OPTIMIZATION
MPC obtains the optimal control quantity by optimizing the performance evaluation index. Different from other traditional control algorithms, this optimization process is

$$A_c = \begin{bmatrix} 0.5975 & 0.0730 & 0.3806 & 0.0244 & -0.0600 & 0.0006 \\ -6.8176 & 0.3844 & 6.0896 & 0.5245 & -1.6121 & 0.0091 \\ 0.0712 & 0.0049 & 0.7967 & 0.0782 & -0.2558 & 0.0010 \\ 1.0777 & 0.1049 & -3.7567 & 0.5087 & -1.4350 & -0.0014 \\ 0.0155 & 0.0012 & 0.0302 & 0.0104 & 0.1096 & -0.0001 \\ 0.0898 & 0.0183 & -0.5293 & -0.0143 & 0.7201 & 0.1513 \end{bmatrix}$$

$$B_c = \begin{bmatrix} -0.00010.0819 \\ -0.00092.3400 \\ 0.00000.3878 \\ 0.00014.1140 \\ 0.00000.8447 \\ 0.0000 - 0.2806 \end{bmatrix}, \quad C_c = C, \quad D_c = D$$

repeated online. The purpose of rolling optimization is to determine the control effect in the future by minimizing the performance indicators (seat acceleration, dynamic deflection, tire dynamic displacement). The goal of the MPC controller is to find the optimal control rate u_k, optimize the ride comfort and stability of the tractor under the constraint conditions, and find the control vector u_k of the minimum value of the objective function at the current time by solving the minimum value of the objective function. At this time, the element in u_k is the active control force F.

The purpose of optimization is to minimize the objective function. The objective function is defined as follows [30]:

$$J = q_1 \cdot \ddot{x}_{se}^2 + q_2 \cdot (x_{se} - x_s)^2 + q_3(x_{us} - q)^2 + r \cdot u^2 \quad (13)$$

where q_1, q_2, q_3 is the weighting coefficient of seat vibration acceleration, suspension dynamic stroke and tire dynamic deflection respectively; r is the weighting coefficient of the control quantity (active control force).

In the optimization design of the seat suspension, according to the characteristics of the controller, in addition to meeting the requirements of the objective function, certain constraints must be met to make the optimization results meet the design requirements. The constraints of optimization problems are usually composed of control variable (u) and state variable (x). Constraints are divided into soft constraints and hard constraints, which cannot violate hard constraints but can violate soft constraints.

(1) The road profile height of the tractor is high on the D and E roads. The MPC controller attenuates the seat vibration by adjusting the actuator. Due to the physical constraints of the vertical movement of the seat suspension system, a strict constraint range is needed to keep the vertical movement of the seat within a certain range and avoid damage to the mechanical structure of the suspension. $|x_{se} - x_s| \leq l_{max}$.

(2) In addition, it is necessary to force the seat acceleration to be the smallest to maximize the ride comfort. This makes the active actuator need to generate a larger active force to attenuate the seat vibration quickly and effectively. For the active actuator, generating a larger active force also means greater energy consumption, and the actuator has a certain power limit. Therefore, the active force needs to be limited to ensure that the controller is in a normal working state. $|F| \leq F_{max}$.

(3) According to the road surface and field working conditions of the tractor, the tractor is prevented from slipping on the muddy and loose soft soil road surface during operation. The static load of the tire is greater than the dynamic load of the tire to ensure that the tire and the ground always have good ground adhesion. $|k_t(x_{se} - x_s)| \leq mg$.

In order to quickly attenuate the vibration, the dynamic deflection of the suspension will also become larger, so it is not a good idea to impose strict constraints on the input and output of the active seat suspension system, because these constraints may conflict with each other, resulting in the inability to solve the optimization problem. Therefore, the output constraint of the seat suspension system is set as a
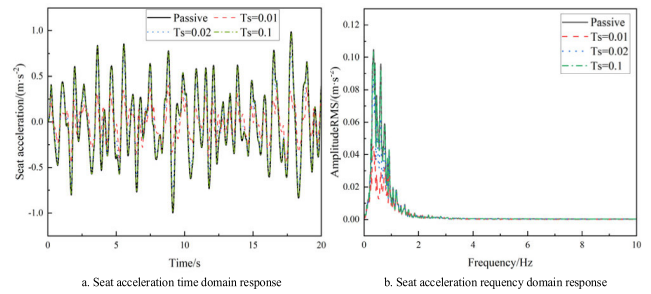

a. Seat acceleration time domain response   b. Seat acceleration requency domain response

FIGURE 8. Simulation results of different sampling time.

soft constraint, and the hard constraint on the input and input change rate is avoided.

In the prediction time domain p, the discrete objective function of k points is established. The purpose of optimization is to minimize the objective function. The quadratic performance index is selected as the rolling optimization objective function. At time t, the following optimization problems are solved.

$$\min J = \sum_{i=1}^{p} Q_i(y(k+i) - y(k+1))^2$$
$$+ \sum_{j=1}^{m} R_j \Delta u^2(k+j-1)^2 \quad (14)$$

where $Q_i = diag(q_1, q_2, q_3)$ and $R_j = r_1$ is the weighted matrix of output variables and control variables respectively.

At each sampling time, the optimization objective is mainly aimed at the dynamic performance of the system in the prediction time domain, and only the first item of the optimal control sequence is applied to the controlled process, that is, the control increment at time k is $\Delta u(k) = d^T(W - Y_0)$, where the variable d can be solved offline in advance. After obtaining new measurements at the next sampling time, the above optimization problem will be re-solved to obtain a new control sequence, so as to achieve rolling optimization.

In order to achieve optimal performance control under actual operating conditions, the constraints of the controller must be considered, so the control quantity and control increment must be constrained.

$$|u(k+i)| \leq u_{max} \quad i = 0, 1, 2 \cdots N - 1$$
$$|\Delta u(k+i)| \leq \Delta u_{max} \quad i = 0, 1, 2 \cdots N - 1 \quad (15)$$

4) FEEDBACK CORRECTION
In order to suppress the control deviation caused by model mismatch or environmental interference, that is, after the controlled object receives the control signal of the predictive controller at time k, the actual output $y(k+1)$ of the controlled system at the time $k + 1$ is not equal to the model predictive output $\hat{y}(k + 1)$, which constitutes a prediction error.

$$e(k + 1) = y(k + 1) - \hat{y}(k + 1) \quad (16)$$

Therefore, at the new sampling time, the actual output of the object is first detected, and this real-time information is
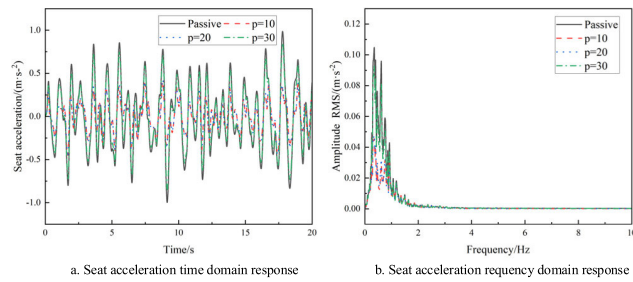
a. Seat acceleration time domain response   b. Seat acceleration requency domain response

FIGURE 9. Simulation results of different prediction time domain.

TABLE 1. MPC active seat suspension performance under different sampling time.

Sampling time	Seat acceleration RMS(m·s⁻²)	Controller one cycle operation time (s)
Passive	0.3942	——
PID	0.3436(↓ 12.84%)	0.0171
Ts=0.01	0.1673(↓ 57.56%)	0.0342(↑ 97.81%)
Ts=0.02	0.3048(↓ 22.68%)	0.0173(↑ 0.90%)
…	…	…
Ts=0.03	0.3900(↓ 1.06%)	0.0163(↓ 4.85%)

TABLE 2. MPC active seat suspension performance under different prediction time domains.

Prediction time domain	Seat acceleration RMS(m·s⁻²)	Controller one cycle operation time (s)
Passive	0.3942	——
P=10	0.1673(↓ 57.56%)	0.0342
…	…	…
P=20	0.1752(↓ 55.56%)	0.0386
…	…	…
P=30	0.3349(↓ 15.04%)	0.0496

used to weight the model-based prediction, and then a new optimization is performed.

$$\tilde{Y}_p = \hat{Y}_p + he(k+1) \qquad (17)$$

where $\tilde{Y}_p = [\tilde{y}(k+1), \tilde{y}(k+1), \cdots , \tilde{y}(k+1)]^T$ is the system output predicted by the system at time $t = (k+1)T$ after error correction; $h = [h_1, h_2, \cdots , h_p]^T$ is the error correction vector, $h_1 = 1$.

The predicted initial value at the next moment is the corrected $\tilde{Y}_p$, and the predicted initial value at time $t = (k+1)T$ is used to predict the future time $t = (k+2)T, \cdots (k+i+1)$ $(i = 1, 2, \cdots p - 1)$.

a. Seat acceleration time domain response   b. Seat acceleration frequency domain response
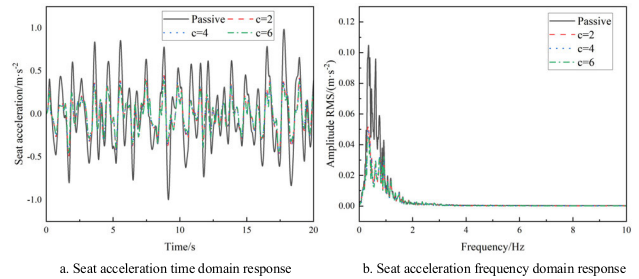
FIGURE 10. Simulation results of different control time domain.

The predicted initial value at the next moment can be obtained:

$$\begin{cases} y_0(k+i) = \tilde{y}(k+i+1) + h_{i+1}e(k+1) \\ y_0(k+p) = \tilde{y}(k+p) + h_p e(k+1) \end{cases} \qquad (18)$$

C. THE INFLUENCE OF MPC PARAMETERS ON THE VIBRATION PERFORMANCE AND CONTROL COST OF SEAT SUSPENSION IS ANALYZED.

As an on-line optimization control algorithm, MPC performs on-line optimization in a finite prediction domain for the state information and constraints of each control cycle of the seat suspension system, so that the controller remains optimal at each moment, which greatly improves the seat suspension vibration reduction performance. However, repeated online optimization will also lead to long control time. Therefore, while improving the performance of seat suspension, the real-time performance and control cost of model predictive control should also be considered. The influence of sampling time, prediction time domain and control time domain on the vibration performance and control cost of seat suspension is analyzed by experiments, and the optimal control effect and control cost are realized. In order to further analyze the MPC controller proposed in this chapter, this section performs simulation analysis through a 1 /4 vehicle model.

1) SAMPLING TIME
The design prediction time domain (p) is 10, the control time domain (c) is 2, and the sampling time (T_s) is 0.01 s, 0.02 s, $\cdots$, 0.1 s, respectively. The simulation results are shown in Fig.8 and Table 1.

Figure 8 (a) and Table 1 show that with the shortening of sampling time, the vertical acceleration of the seat becomes smaller and the control effect is better. This is because the shorter the sampling time. The smaller the gap between the discrete model and the actual model, the faster the controller responds to changes in interference, and the more accurate the control. At the same time, it is noted that as the sampling time is shortened, the discrete model is more accurate, resulting in too much calculation load, and the operation time of the controller becomes longer, which has a certain impact on the control timeliness. When $T_s = 0.02s$, compared with PID control, the control effect of MPC is improved by 22.68%, while the control time consumption is only increased by 0.90 %.

TABLE 3. MPC active seat suspension performance under different control time domain.

Prediction time domain	Seat acceleration RMS(m · s⁻²)	Controller one cycle operation time (s)
Passive	0.3942	——
…	…	…
c=2	0.1673(↓57.56%)	0.0342
...	…	…
c=4	0.1612(↓ 59.11%)	0.0396
…	…	…
c=6	0.1586(↓59.77%)	0.0418
…	…	…

Figure 8 (b) shows that when $T_s = 0.01$s and 0.02s, the ride comfort is greatly improved in the low frequency range (0-2Hz).

2) PREDICTION TIME DOMAIN

The design control time domain (c) is 2, the sampling time (T_s) is 0.01 s, and the prediction time domain (p) is 10,12, · · · ·, 30. The simulation results are shown in Figure 8 and Table 2.

Figure 9 (a) and Table 2 show that when the sampling time and control time domain are fixed and the prediction time domain increases gradually, the control effect of MPC becomes worse. This is because the control time domain is unchanged, and the prediction time domain is added separately. The controller will consider more system state trend changes, resulting in large errors and reduced control accuracy. At the same time, it is noted that the one-cycle operation time of the controller becomes longer with the increase of the prediction time domain.

Figure 9 (b) shows that when the predicted time domain $p = 10$ and 20, the ride comfort is greatly improved in the low frequency range.

3) CONTROL HORIZON

The design sampling time (T_s) is 0.01 s, the prediction time domain (p) is 10, and the control time domain (c) is 1, 2, · · ·, 10. The simulation results are shown in Fig.9 and Table 3.

Figure 10 (a, b) and Table 3 show that when the sampling time and prediction time domain are fixed and the control time domain is gradually increased, the control effect is gradually improved, but not obvious. This is because the larger the control time domain, the more sets of solutions can be solved, but the feedback correction controller of MPC only applies the first element of the control increment to the system. At the same time, it is noted that the one-cycle operation time of the controller becomes longer with the increase of the prediction time domain.

Considering the control effect and time cost, the MPC parameters are selected: sampling time $T_s = 0.02$, prediction time domain $p = 10$, control time domain $c = 2$.

4) WEIGHTED MATRIX OF OUTPUT VARIABLES AND CONTROL VARIABLES

As the output variable weighting matrix Q_i and the control variable weighting matrix R_j of the design parameters, the basic principles of selection are as follows:

(a)When the fast response performance of the system needs to be improved, it can be achieved by reducing R_j (or increasing Q_i);

(b)In order to effectively suppress the control quantity, reduce the control cost and improve the steady-state performance of the system, it can be achieved by increasing R_j (or decreasing Q_i).

(c)The effects of weighted matrix Q_i and R_j are mutually restricted.

D. MULTI-OBJECTIVE OPTIMIZATION OF MPC ACTIVE SEAT SUSPENSION CONTROL SYSTEM

In the previous section, the influence of the main parameters and constraints of MPC on the control effect and cost is analyzed. The optimization problem of seat suspension should be viewed from the global point of view, and the optimization idea should be run through the design process of the controller, so that the optimization effect can be more obvious. Based on the MPC parameters determined above, the weight matrix of the controller is optimized and analyzed. Design reasonable variables, formulate accurate constraints, find the objective function of the system, and comprehensively analyze the optimization problem. The specific contents are as follows:

The optimal selection of the output variable weight parameter Q_i and the input variable change rate weight parameter R_j of the MPC controller is an important factor for the MPC controller to achieve good control performance. The control performance and stability are determined by the four parameters $K = [Q_i, R_j] = [q_1, q_2, q_3, r]$ in the model predictive controller. By selecting these parameters to meet multiple objectives and constraints, the multi-objective optimization design problem can be transformed into [31]:

$$\min_{K \in N} \{F(K)\} = \min_{K \in N} \{f_1, f_2, f_3\} \qquad (19)$$

where K is the model predictive controller parameter; f_1, f_2, f_3 is the optimization goal.

Before optimizing the seat suspension system, the following control objectives are set according to the system performance requirements.

1) SEAT VERTICAL ACCELERATION

The index of vibration to ride comfort is mainly measured by the vibration acceleration of the driver 's body in the vertical direction, and the vertical acceleration of the seat should be
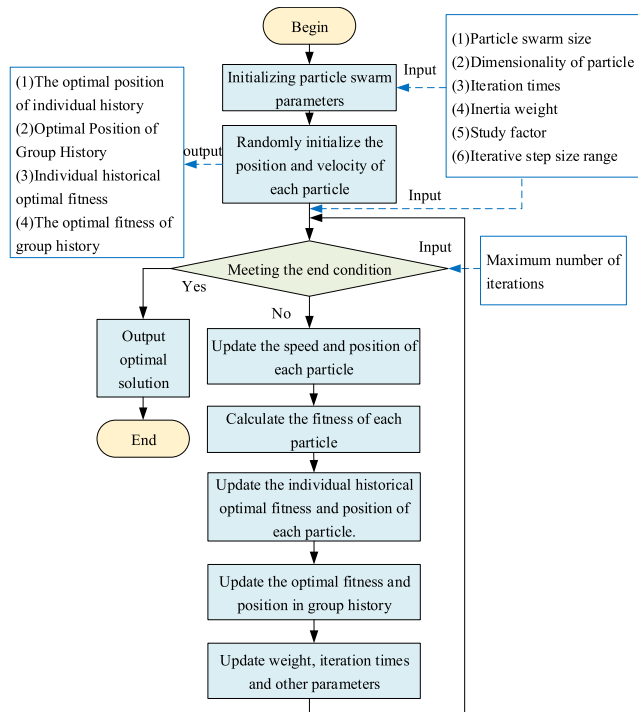
FIGURE 11. Particle swarm algorithm flow chart.

TABLE 4. Performance comparison and time cost comparison of different optimization methods.

Different methods	Performance index	Time cost
	Performance and cost improvement（%）	
GA-MPC	32.36	40.45
CSOA-MPC	54.54	47.25
PSO-MPC	53.42	68.69

as small as possible. The calculation formula is as follows:

$$a_w = [\frac{1}{T}\int_0^T a_w^2(t)dt]^{\frac{1}{2}} \tag{20}$$

where T is the analysis time of vibration.

2) DYNAMIC DEFLECTION OF SEAT SUSPENSION
The dynamic deflection of seat suspension is an important index of ride comfort and suspension safety, which is related to its limit stroke. The value is the difference between the displacement of the upper surface of the seat and the displacement of the cab floor.

$$\Delta x_1 = x_{se} - x_s \tag{21}$$

where x_{se} is the displacement of the upper surface of the seat; x_s is the displacement of the cab floor.

3) TIRE DISPLACEMENT
The driving stability index of the tractor in the vertical direction of various complex roads is mainly measured by the

dynamic displacement between the wheel and the ground, which is the difference between the tire displacement and the road excitation displacement.

$$\Delta x_2 = x_{us} - q \tag{22}$$

where x_{us} is the tire displacement; q is road excitation displacement.

Therefore, the designed objective function is:

$$\begin{cases} f_1 = \sqrt{\dfrac{1}{n}\sum_{i=1}^{n}\ddot{x}_{se}^2(t_i)} \\ f_2 = \sqrt{\dfrac{1}{n}\sum_{i=1}^{n}[x_{se}(t_i) - x_s(t_i)]^2} \\ f_3 = \sqrt{\dfrac{1}{n}\sum_{i=1}^{n}[x_{us}(t_i) - q(t_i)]^2} \end{cases} \tag{23}$$

where f_1, f_2, f_3 is the root mean square of seat vertical acceleration, seat suspension dynamic stroke and tire dynamic displacement respectively.

The core of the seat suspension optimization problem is to make the objective function values as small as possible under the constraint conditions. The model predictive controller control parameters are selected as design variables to establish a multi-objective optimization problem. The better effect fitness can be obtained by directly transforming the multi-objective function into the fitness function. The value of the function function measures the position of the particles. The fitness function can be expressed as:

$$Fit(K) = \min(f_1, f_2, f_3) \tag{24}$$

The particle swarm optimization algorithm has the following advantages: (1) PSO has no crossover and mutation operations, and relies on particle speed to complete the search, and the search speed is fast; (2) There are few parameters to be adjusted, the structure is simple, and it is easy to implement in the project. For the seat suspension system, MPC active control is more complex, so this advantage of PSO becomes our first choice [32]. MPC is applied to active seat suspension control, the effect is good enough, but the control is more complex and time-consuming, so the control cost and timeliness become our goal. The optimization of active seat suspension system is a low-dimensional three-dimensional optimization problem. PSO is suitable for low-dimensional optimization, which is what we need. Compared with other bionic algorithms, it does not require coding, no crossover and mutation operations, and particles can converge to the optimal solution faster only through internal velocity updates. Therefore, we apply the particle swarm optimization algorithm to solve the low-dimensional optimization problem of MPC active seat suspension parameters and solve the MPC controller parameters faster.

Compare P-MPC with classical genetic algorithm (GA) and search optimization algorithm (CSOA). Set the weights

TABLE 5. Tractor seat suspension simulation parameter table.

Model parameter	Value	Unit
Reed mass (body part) m_s	400	Kg
Unsprung mass (tire mass) m_{us}	40	Kg
Seat quality m_{se}	80	Kg
Seat damping coefficient c_{se}	300	N·s·m^{-1}
Body damping coefficient c_s	1500	N·s·m^{-1}
Seat stiffness k_{se}	8000	N·m^{-1}
Body stiffness k_s	16000	N·m^{-1}
Tire stiffness k_t	160000	N·m^{-1}

a. Road excitation under different grade pavement   b. Road excitation at different speeds
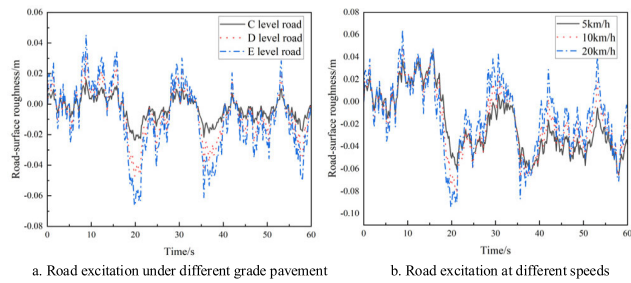
FIGURE 12. Road excitation simulation at different pavement grades and vehicle speeds.

of tire dynamic displacement, suspension dynamic displacement, and seat acceleration to 0.2, 0.3, and 0.5 respectively. Table 4 shows the performance comparison and time cost comparison results of different optimization methods. In terms of performance indicators, GA optimization is the worst, and PSO and CSOA have significantly improved system performance, with CSOA only 1.12% higher than PSO. It is worth noting that in terms of time cost, GA is the worst, and PSO and CSOA have a significant improvement in time, with PSO being 21.44% higher than CSOA. We can see that PSO has the characteristics of fast convergence speed, simple execution process, fewer solving parameters, and low computational complexity. Overall, its overall performance is superior to GA and CSOA. Especially for the three-dimensional seat vibration reduction optimization problem in this article, the optimization effect and performance are good while ensuring the important premise of time cost.

The particle swarm optimization process is shown in Figure 11. In the D-dimensional space, there are N particles, $X_i = (X_{i1}, X_{i2}, \cdots, X_{iD})$,which represent the position of the i th particle, and bring X_i into the fitness function to obtain the fitness value of the fitness function. $V_i = (V_{i1}, V_{i2}, \cdots, V_{iD})$ denotes the velocity of the i particle. $V_{best\ i} = (P_{i1}, P_{i2}, \cdots, P_{iD})$ represents the best position experienced by the i particle, and $g_{best\ i} = (g_1, g_2, \cdots, g_D)$

represents the best position experienced by the population. The d-dimensional velocity update formula of the i particle is [33], [34]:

$$V_{id}^{k+1} = \omega V_{id}^k + c_1 r_1(P_{id}^k - X_{id}^k) + c_2 r_2(P_{gd}^k - X_{id}^k) \quad (25)$$

The d-dimensional position update formula of the i particle is:

$$X_{id}^{k+1} = X_{id}^k + V_{id}^{k+1} \quad (26)$$

where V_{id}^k is the d -dimensional component of the velocity vector of the i particle in the k -th iteration.; c_1, c_2 is the acceleration constant; r_1, r_2 is two random functions; ω is inertia weight; X_{id}^k is the position of the k-th iteration particle; P_{id}^k is the d -dimension of the individual extreme value i variable in the k-th iteration; P_{gd}^k is the d -dimension of the global optimal solution of the k -th iteration.

The parameters of the particle swarm optimization algorithm are set as follows: the initial population number is set to 100, the maximum number of iterations is 200, the inertia weight $\omega_{max} = 0.8, \omega_{min} = 0.5$, the acceleration factor $c_1 = c_2 = 2$, the simulation time is 20 s, and the optimized $[q_1, q_2, q_3, r] = [0.52, 256, 214, 0.005]$.

IV. SIMULATION AND EXPERIMENTAL ANALYSIS
A. SYSTEM SIMULATION AND APPLICATION RESULTS ANALYSIS
After defining the system model, defining the input and output of MPC and setting the parameters of model predictive controller, the simulation model of the system is established and analyzed. Build the simulation model of the whole system. Model parameters are shown in Table 5.

In actual road conditions, the efficiency of the seat suspension is evaluated by random input of the road surface. Most of the periodic vibration and high frequency vibration caused by engine vibration have been isolated by the seat system. This paper mainly studies the random vibration in the low frequency range caused by ground uneven excitation. According to 'vehicle vibration input-road surface roughness representation', the time domain expression of road roughness can be expressed by the following formula [27].

$$\dot{q}(t) = -2\pi n_1 uq(t) + 2\pi n_0 \sqrt{G_q(n_0)u}w(t) \quad (27)$$

where $q(t)$ is road displacement; G_0 is the road roughness coefficient, $G_0 = 1.024 \times 10^{-3}$ under D-class road surface, $G_0 = 4.096 \times 10^{-3}$ under E-class road surface; n_1 is the lower cut-off frequency, $n_1 = 0.01m^{-1}$; w is Gaussian white noise with mean value of 0.

According to the actual driving conditions of the tractor (including the transfer and transportation of the tractor) and the road roughness of the field operation, the C and D road surfaces with the speed of 20km / h are selected to simulate the transfer and transportation of the tractor in the non-road field rugged road year, and the D and E road surface simulation tractors with the speed of 10km / h are selected to analyze the field operation, and the road roughness time
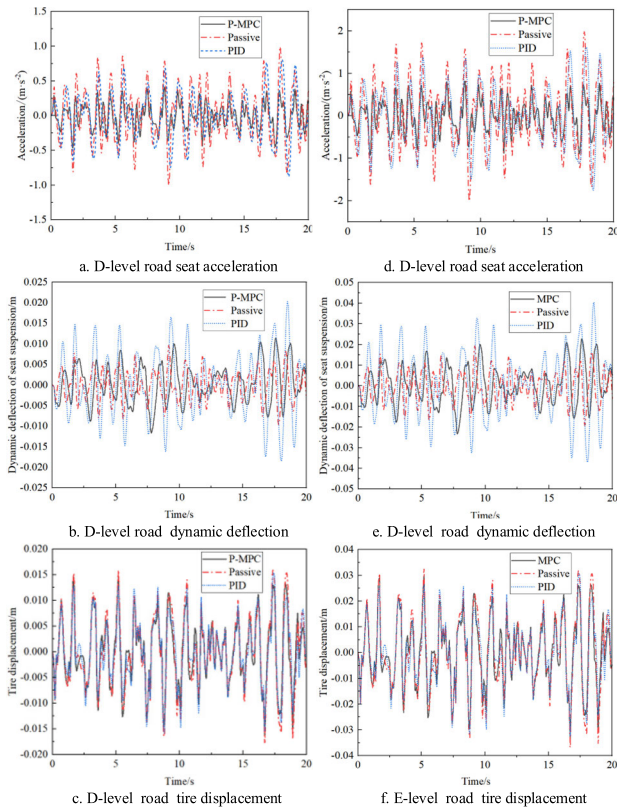
FIGURE 13. Suspension performance comparison of different control methods under different grade road types.

TABLE 6. Performance comparison of seat suspension with different control methods.

Performance index	Root mean square value (RMS)		
	Passive	PID control	P-MPC control
Seat acceleration/(m·s^{-2})	0.3942	0.3436	0.1873
Dynamic deflection/mm	1.98	3.04	2.693
Tire displacement/mm	2.94	2.38	1.05

FIGURE 14. Performance comparison of seat suspension with different control methods under different driving speeds.
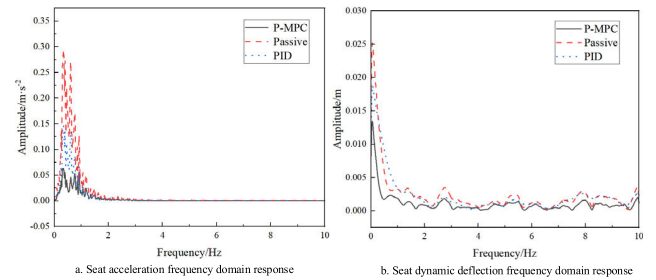
FIGURE 15. Fourier Comparison Curve of Seat Suspension.

TABLE 7. Performance index comparison of P-MPC seat suspension system under different load mass.

Performance index	Root mean square value (RMS)		
	m_{se}=80kg	m_{se}=100kg	Rate of change
Seat acceleration/(m·s^{-2})	0.18732	0.2087	-11.4%
Dynamic deflection/mm	2.693	2.448	+9.12%
Tire displacement/mm	1.052	1.137	+8.1%

domain model is built, as shown in Figure 12. The sampling time is set to 0.005 s and the simulation time is set to 60 s.

In order to verify the effectiveness of the control and algorithm, the active seat suspension system is simulated and analyzed. Figure 13-14 is the time-domain comparison curve of each comfort index, and Figure 15 is the Fourier comparison curve. The root mean square (RMS) values of each index are shown in Table 5.

Figure 13-14 shows that at different speeds and different levels of road conditions. In terms of human-seat vertical vibration acceleration and tire dynamic displacement, the MPC with optimized control parameters (P-MPC) has the best control effect. For the dynamic deflection of the seat suspension, P-MPC and PID are worse than the passive seat suspension. This is due to the characteristics of active control.
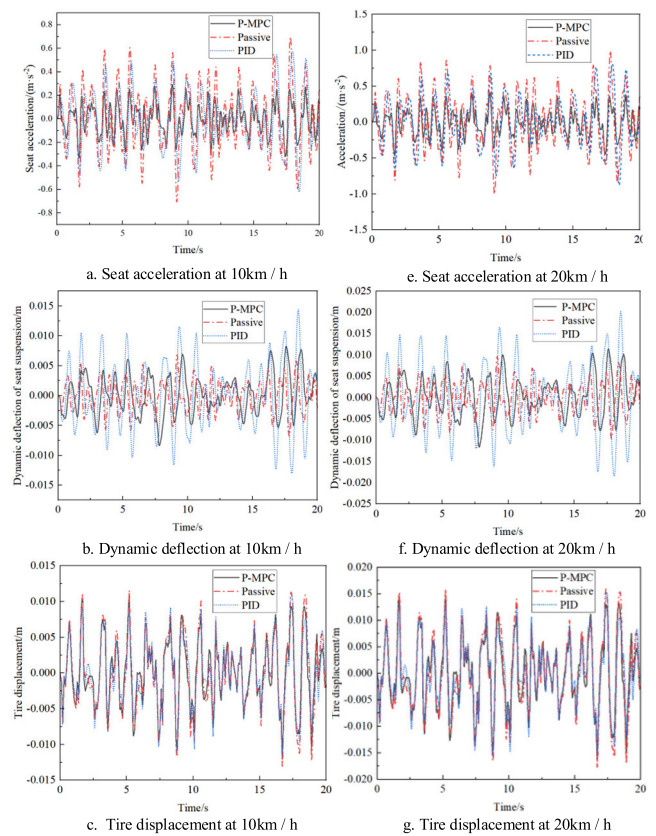
In order to achieve the optimal performance of one target, other target performance is reduced. In order to achieve the optimal vibration reduction effect, the active seat suspension sacrifices the displacement of the seat suspension, resulting in
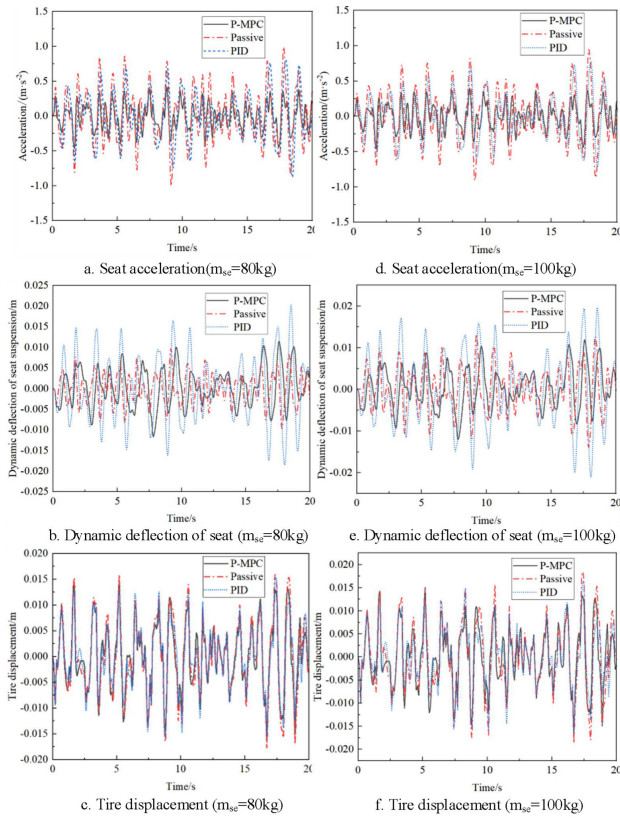
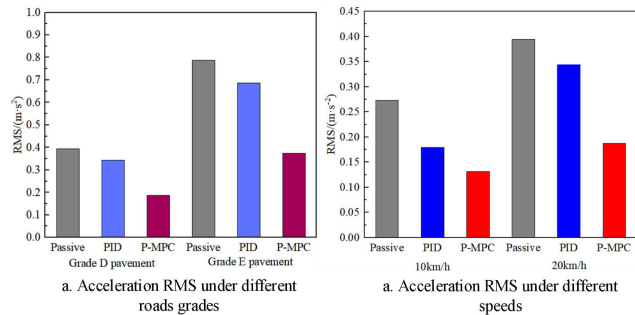**FIGURE 16. Performance comparison of seat suspension with different control methods under different load mass.**

FIGURE 17. Suspension performance comparison of different control methods under different grade road types.

FIGURE 18. The active power required by different control schemes under D-level and E-level road types.
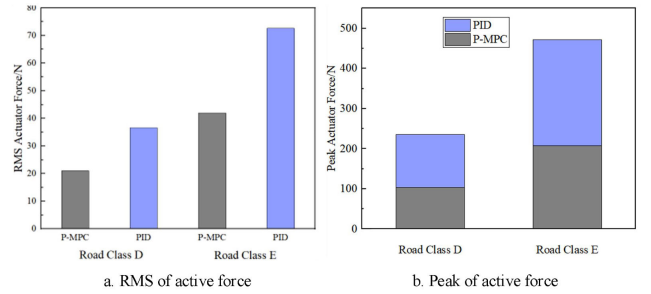
FIGURE 19. The RMS value of active force and the peak force of actuator under different.

an increase in dynamic deflection, but the dynamic deflection is still within the limit.

Figure 15 shows that the optimized P-MPC active seat suspension effectively reduces the acceleration and dynamic deflection of the seat in the low frequency range of the body resonance frequency range (1 Hz ∼ 1.5 Hz) and the low frequency range where the human internal organs are prone to resonance and the seat surface is most sensitive (4 H ∼ 10 Hz), thereby reducing the passenger 's inadaptability and improving the ride comfort.

Table 6 shows that compared with passive control, the RMS of seat vibration acceleration is reduced by 52.5 %, and the RMS of tire dynamic displacement is reduced by 64.3 %. Compared with PID, it is reduced by 45.5 % and 55.9 % respectively. The P-MPC effectively improves the ride
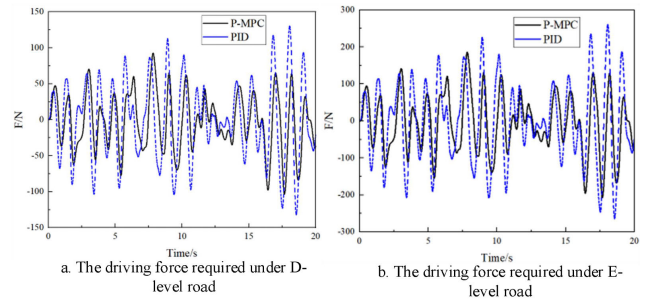
comfort of the tractor, enhances the grasping ability of the tractor tire under various complex road surfaces and driving conditions, and improves the driving stability of the tractor.

In order to consider the dynamic response of the seat suspension system to the change of load mass, the influence of different load mass (m_{se}) on the vibration reduction performance is compared and analyzed. In the dynamic model of tractor active seat suspension system established in Section I-A of this paper, m_{se} is the combined mass of human and seat. Figure 16 shows the simulation results of the system under different load mass. With the increase of load mass, the vibration evaluation index of human comfort decreases.

Table 7 shows that the range of human comfort index of P-MPC active seat suspension system is very small when the load mass changes. As the load mass increases, the seat vibration acceleration increases by 11.4%, the seat suspension dynamic deflection decreases by 9.12%, and the tire dynamic displacement decreases by 8.1%. P-MPC has better vibration control characteristics and robustness to load mass changes. It has good dynamic performance and can solve problems such as sudden interference.

As the most important one of the three performance indexes of seat suspension, the vertical vibration acceleration of human-seat is analyzed and compared separately. Figure 17 shows the root mean square values of the seat acceleration of the system under different road types and different speeds. In the case of D and E roads, the seat vibration acceleration amplitude of P-MPC is 52.49 % lower than that of PID, and 45.49 % lower than that of passive control. At the speed of 10km / h and 20km / h, compared with PID, the amplitude of seat vibration acceleration of P-MPC is reduced
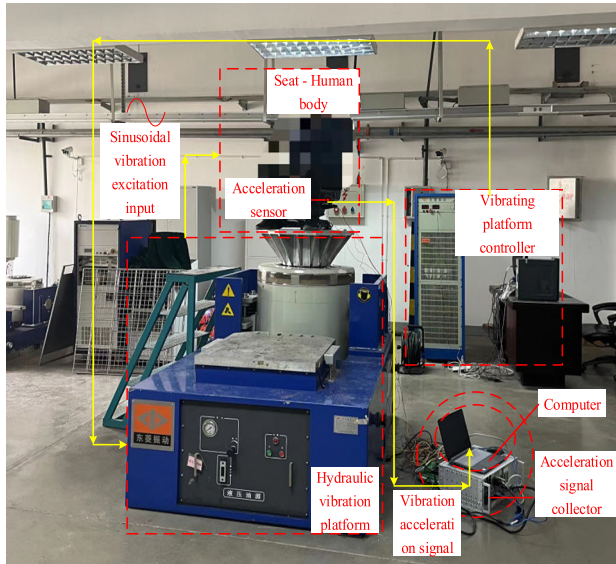
FIGURE 20. Seat vibration test.

a. Comparison curve of seat acceleration (m_{se} = 80kg)

c. Comparison curve of seat acceleration (m_{se} = 100kg)

b. Seat acceleration RMS Fourier contrast curve(m_{se} = 80kg)

d. Seat acceleration RMS Fourier contrast curve(m_{se} = 100kg)

FIGURE 21. Vibration test results of seats with different human-seat combinations.

by 51.90 %, and compared with passive control, it is reduced by 24.43 %. The P-MPC effectively improves the vibration reduction effect, thereby reducing the impact of the severe impact vibration of the tractor on the driver 's physical and mental health when driving on complex field roads.

Figure 18 shows the active force required for the seat suspension system of P-MPC and PID under the two road types of D and E, and the active force has obvious changes on the two road types. Figure 19 shows the root mean square value and peak value of the active force required by the P-MPC and PID active seat suspension systems. As the road grade increases, the root mean square value and peak value of the active force required by the system increase. Table 7 shows the specific analysis results.

Table 8 shows that compared with PID active control, the P-MPC active seat suspension system reduces the peak active force of the actuator by 22.94 % and 21.47 % respectively under D and E road types. The root mean square value of the active force was reduced by 42.83% and 45.01%, respectively. On the two types of roads, the actuator active force of PID and P-MPC control schemes is within a specific constraint range. The reduction of the active force reduces the current of the actuator and the rated power, which in turn makes the physical size of the actuator smaller and the weight lower. P-MPC reduces the power consumption of the active seat suspension on the basis of improving the comfort of the seat suspension.

B. EXPERIMENTAL ANALYSIS

Figure 20 shows the test device to study and analyze the dynamic performance and vibration reduction effect of the seat suspension system. The test platform includes electro-hydraulic vibration platform, vibration platform controller, computer, vertical vibration signal sensor and vibration signal collector. The tractor seat is fixed on the vibration platform by detachable link. Under the action of the platform
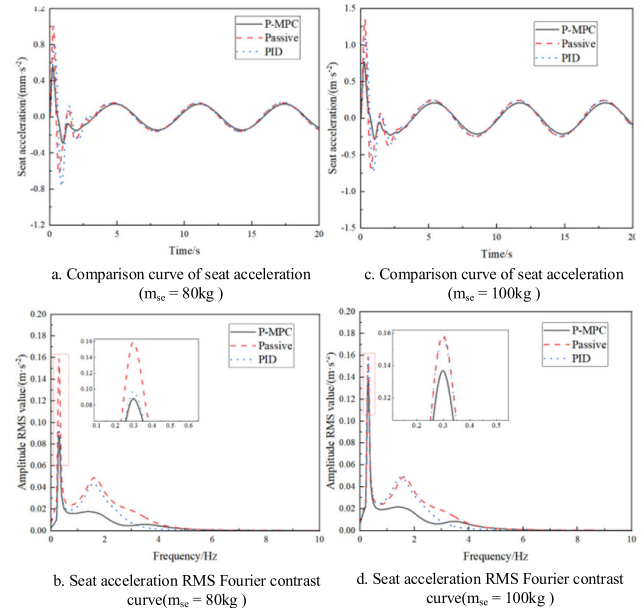
TABLE 8. Comparison of root mean square value and peak value of active power of P-MPC and PID under different pavement types.

Pavement types	RMS of active force /N			Peak of active force/N		
	PID control	P-MPC control	Rate of change	PID control	P-MPC control	Rate of change
Grade D pavement	36.68	20.97	42.83%	134.69	103.79	22.94%
Grade E pavement	72.63	41.94	45.01%	264.07	207.41	21.47%

controller, the electro-hydraulic vibration platform generates sinusoidal excitation. The vibration signal sensor is installed on the upper surface of the seat to measure the acceleration signal on the upper surface of the seat. The acceleration signal is transmitted to the vibration signal collector, and finally the vibration test results are displayed on the computer.

In this test, the human-seat combination mass m_{se} was divided into light (80 kg) and heavy (100 kg). The electro-hydraulic vibration platform is input to the human-seat system with an amplitude of 0.2 m, a frequency of 1 rad/s sinusoidal vibration signal, and each measurement is 20 s. Figure21 (a, c) shows the seat acceleration curve under sinusoidal vibration excitation input, and Figure 21(b, d) shows the Fourier comparison curve.

Periodicity and seasonality are typical characteristics of agricultural production. Tractor drivers are subjected to low-frequency (1-8Hz) high-intensity vibration for a long time. The test results show that the seat acceleration of the P-MPC active seat suspension is significantly reduced in the frequency range of 0-10 Hz. In the low frequency range of body resonance (1 Hz $\sim$ 1.5 Hz) and human internal organs prone to resonance (4 Hz $\sim$ 12.5 Hz), P-MPC effectively reduces the acceleration of the seat compared to other methods, thereby

reducing the impact of the severe impact vibration generated by the tractor on the driver's physical and mental health.

The P-MPC active seat suspension achieves the highest efficiency of active control at the resonance frequency (about 0.3 Hz), and the harmful vibration at this frequency is reduced by about 43.75 %. Under different load masses, the P-MPC active seat suspension system has strong robustness. In the frequency range of 0-4 Hz, the active force generated by the actuator effectively attenuates the seat vibration. At higher frequencies (greater than 4 Hz), the shock absorber force and spring force are dominant. The test results show that the model predictive control has better vibration control characteristics under the premise of less energy consumption and timeliness.

V. CONCLUSION

(1) The simulation and experimental results show that under different test conditions, P-MPC significantly attenuates the seat vibration and has good dynamic characteristics. For the vertical axial vibration of the seat support surface, in the low frequency range where the human body is most sensitive and the internal organs are prone to resonance, the active force generated by the P-MPC active seat suspension effectively reduces the seat acceleration, thereby improving the tractor. The severe vibration generated when driving on complex field roads has an impact on the driver's physical and mental health.

(2) Within the defined constraint range, the inner-loop current hysteresis comparison control realizes the accurate tracking of the active force required for the outer-loop control, and the peak and root mean square values of the active force of the actuator are significantly reduced, which reduces the system power consumption.

(3) The influence of MPC controller parameters on system performance and response characteristics is analyzed through experiments, and the weight matrix of MPC controller is optimized to ensure the control timeliness and achieve the optimal comprehensive performance. The results of this study provide a theoretical basis for subsequent research and have certain practical significance.

REFERENCES

[1] Y. Yang, S. K. Cheng, and J. Qi, "Design and experiment of automatic leveling system for agricultural machinery seat based on ergonomics," *Trans. Chin. Soc. Agricult. Machinery*, vol. 53, no. 6pp. 434–444, 2022.

[2] Q. Wang, Y. Huo, Z. Xu, W. Zhang, Y. Shang, and H. Xu, "Effects of backrest and seat-pan inclination of tractor seat on biomechanical characteristics of lumbar, abdomen, leg and spine," *Comput. Methods Biomech. Biomed. Eng.*, vol. 26, no. 3, pp. 291–304, Feb. 2023.

[3] M. Chen, Q. H. Zhao, and J. Z. Yang, "Research on the vibration response of three-dimensional sitting human model considering seat design," *J. Qingdao Univ., Eng. Technol. Ed.*, vol. 37, no. 4, pp. 49–60, 2022.

[4] G. Ruitao, W. Yang, Y. Zhou, J. Hong, L. Zhixiang, and S. Jian, "Tractor driving seat suspension system research status and strategies in China: A review," *IFAC-PapersOnLine*, vol. 51, no. 17, pp. 576–581, 2018.

[5] S. A. Adam and N. A. A. Jalil, "Vertical suspension seat transmissibility and SEAT values for seated person exposed to whole-body vibration in agricultural tractor preliminary study," *Proc. Eng.*, vol. 170, pp. 435–442, Jan. 2017.

[6] Q. Zhao and N. Zhang, "Design of canopy backstepping controller for vehicle active seat suspension," *Noise Vib. Control*, vol. 38, no. 4, pp. 12–17, 2018.

[7] X. L. Wang, J. Y. Huang, and H. F. Lv, "H∞ optimal control of vehicle semi-active seat suspension system based on sliding mode observer," *Vib. Shock*, vol. 41, no. 13, pp. 246–251, 2022.

[8] S. J. Sha, Z. G. Wang, and H. P. Du, "Research on the performance of semi-active seat suspension system of vehicle using magnetorheological damper," *Mech. Des. Manuf.*, vol. 370, no. 12, pp. 48–53, 2021.

[9] S. Ma, H. Jiang, and X. L. Guo, "Research on active seat suspension system based on low-pass filter PID control," *J. Liaocheng Univ., Natural Sci. Ed.*, vol. 35, no. 6, pp. 1–7, 2023.

[10] G. G. Luan, P. F. Liu, and D. H. Ning, "Semi-active vibration control of seat suspension equipped with a variable equivalent inertance-variable damping device," *Machines*, vol. 11, no. 2, p. 284, 2023.

[11] O. Munyaneza and J. W. Sohn, "Modeling and control of hybrid MR seat damper and whole body vibration evaluation for bus drivers," *J. Low Freq. Noise, Vibrat. Act. Control*, vol. 41, no. 2, pp. 659–675, Jun. 2022.

[12] D. X. Phu, V. Mien, and S.-B. Choi, "A new switching adaptive fuzzy controller with an application to vibration control of a vehicle seat suspension subjected to disturbances," *Appl. Sci.*, vol. 11, no. 5, p. 2244, Mar. 2021.

[13] J. H. Lee, "Model predictive control: Review of the three decades of development," *Int. J. Control, Autom. Syst.*, vol. 9, no. 3, pp. 415–424, Jun. 2011.

[14] J. Narayan, S. A. Gorji, and M. M. Ektesabi, "Power reduction for an active suspension system in a quarter car model using MPC," in *Proc. IEEE Int. Conf. Energy Internet (ICEI)*, Aug. 2020, pp. 140–146.

[15] I. Maciejewski, S. Glowinski, and T. Krzyzynski, "Active control of a seat suspension with the system adaptation to varying load mass," *Mechatronics*, vol. 24, no. 8, pp. 1242–1253, Dec. 2014.

[16] M. Papadimitrakis and A. Alexandridis, "Active vehicle suspension control using road preview model predictive control and radial basis function networks," *Appl. Soft Comput.*, vol. 120, May 2022, Art. no. 108646.

[17] K. Huang, F. Yu, and Y. C. Zhang, "Design of model predictive controller for electromagnetic active suspension," *J. Shanghai Jiaotong Univ.*, vol. 44, no. 11, pp. 1619–1624, 2010.

[18] Q. Zhao and J. X. Yin, "Predictive control of vehicle electro-hydraulic active suspension," *J. Wuhan Univ. Technol., Traffic Sci. Eng. Ed.*, vol. 38, no. 5, pp. 979–983, 2014.

[19] F. Yu, *Vehicle Dynamics and Control*. Beijing, China: People's Commun. Press, 2003, pp. 23–24.

[20] M. Al-Ashmori and X. Wang, "A systematic literature review of various control techniques for active seat suspension systems," *Appl. Sci.*, vol. 10, no. 3, p. 1148, Feb. 2020.

[21] Y. W. Yu, L. L. Zhao, and C. C. Zhou, "Design and analysis of vehicle seat suboptimal control active suspension," *J. Beijing Univ. Posts Telecommun.*, vol. 44, no. 3, pp. 87–93, 2021.

[22] H. Du, W. Li, and N. Zhang, "Integrated seat and suspension control for a quarter car with driver model," *IEEE Trans. Veh. Technol.*, vol. 61, no. 9, pp. 3893–3908, Nov. 2012.

[23] A. Kuznetsov, M. Mammadov, I. Sultan, and E. Hajilarov, "Optimization of a quarter-car suspension model coupled with the driver biomechanical effects," *J. Sound Vibrat.*, vol. 330, no. 12, pp. 2937–2946, Jun. 2011.

[24] X. J. Xia, D. H. Ning, and M. Y. Zheng, "Design of integrated suspension control system based on TS fuzzy model and disturbance observer," *J. Hefei Univ. Technol., Natural Sci. Educ.*, vol. 44, no. 1, pp. 21–30, 2021.

[25] Y. L. Yang, "Research on permanent magnet synchronous linear motor drive control based on model predictive control," Southeast Univ., Jiangsu, China, Tech. Rep., 2021, pp. 9–13.

[26] S. Y. Wang, "Design and research of permanent magnet synchronous linear motor for electromagnetic active suspension," Beijing Inst. Technol., Beijing, China, Tech. Rep., 2017, pp. 13–20.

[27] X. L. Chen, H. Song, and S. X. Zhao, "Ride comfort investigation of semi-active seat suspension integrated with quarter car model," *Mech. Ind.*, vol. 23, p. 18, Feb. 2022.

[28] J. W. Gong, *Model Predictive Control of Driverless Vehicle*. Beijing, China: Beijing Inst. Technol. Press, 2020, pp. 57–60.

[29] B. E. Durmaz, B. Kaçmaz, İ. Mutlu, and M. Turan Söylemez, "Implementation and comparison of LQR-MPC on active suspension system," in *Proc. 10th Int. Conf. Electr. Electron. Eng. (ELECO)*, Dec. 2017, pp. 828–835.

[30] F. R. Kou, T. Fang, and Q. Ren, "Research on inner and outer loop control of linear motor active suspension," *J. Syst. Simul.*, vol. 30, no. 7, p. 2615, 2018.

[31] K. M. Gao, Z. H. Guo, and C. C. Ma, "Design of sliding mode controller for active seat suspension based on multi-objective particle swarm optimization," *Sci. Technol. Eng.*, vol. 19, no. 29, pp. 319–326, 2019.

[32] C. S. Zhan and L. Q. Su, "PID control strategy of active suspension based on particle swarm optimization," *Sci. Technol. Eng.*, vol. 22, no. 10, pp. 4180–4186, 2022.

[33] D. H. Ning, Z. J. Jia, and M. M. Dong, "Research progress of vehicle seat suspension damping system," *J. China Jiliang Univ.*, vol. 29, no. 2, pp. 113–120, 2018.

[34] L. X. Zhang, "Rolling horizon control of vehicle active suspension based on particle swarm optimization," *Agricult. Equip. Vehicle Eng.*, vol. 58, no. 12, pp. 37–41, 2020.
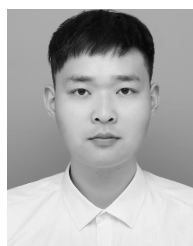
XIAOLIANG CHEN (Member, IEEE) received the B.S. degree in agricultural mechanization and automation from the Henan University of Science and Technology, Luoyang, China, in 2009, the M.S. degree in mechanical design and theory from Zhejiang Sci-Tech University, Hangzhou, China, in 2013, and the Ph.D. degree in vehicle engineering from the Henan University of Science and Technology, in 2023. His research interests include fault diagnosis of agricultural machinery and NVH.

SIXIA ZHAO (Member, IEEE) received the B.S. degree in mechanical engineering and automation from Henan Polytechnic University, Jiaozuo, China, in 2013, and the M.S. degree in mechanical engineering and the Ph.D. degree in vehicle engineering from the Henan University of Science and Technology, Luoyang, China, in 2018 and 2022, respectively. Since 2022, he has been a Lecturer with the College of Vehicle and Traffic Engineering, Henan University of Science and Technology. His research interests include the fault diagnosis of agricultural machinery and new transmission system of agricultural vehicles.

ZHI GAO (Member, IEEE) received the B.S. degree in vehicle engineering from the Huanghe Science and Technology College, Zhengzhou, China, in 2017. He is currently pursuing the Master of Engineering degree in vehicle engineering with the Henan University of Science and Technology, Luoyang, China. His research interest includes hybrid power systems in agricultural machinery.

GUANGCHAO QU (Member, IEEE) received the B.S. degree in vehicle engineering from Zhengzhou Technology and Business University, Zhengzhou, China, in 2017. He is currently pursuing the master's degree in vehicle engineering with the Henan University of Science and Technology, Luoyang, China. His research interest includes NVH in agricultural machinery.

MENGNAN LIU (Member, IEEE) received the Ph.D. degree from the Xi'an University of Technology, in 2021. He is currently the Product Management Director of YTO Group Corporation. In the meantime, he is also the Deputy Director of the National Key Laboratory for Power Equipment of Intelligent Agricultural Machinery and a General Vice Secretary of Youth Committee with the Chinese Society for Agricultural Machinery. His research interest includes novel power system for agricultural machinery and its intelligent control technique.

LIYOU XU (Member, IEEE) received the B.S. degree in mechanical manufacturing technology and equipment from the Jiaozuo Institute of Technology, Jiaozuo, China, in 1998, the M.S. degree in vehicle engineering from the Luoyang Institute of Technology, Luoyang, China, in 2018, and the Ph.D. degree in vehicle engineering from the Xi'an University of Technology, Xi'an, in 2007. Since 2013, he has been a Professor with the College of Vehicle and Traffic Engineering, Henan University of Science and Technology, Luoyang. His research interests include new transmission theory and control technology, vehicle performance analysis method and simulation technology, and low-speed electric vehicle transmission technology.

• • •